Floating Offshore Wind Turbine Wake Structure During Surge Motion Using an Actuator Line Model

Q. Graham*, A. Shahrokhi*, S. Malkeson*, M. Seddighi*
Corresponding author: Q.graham2022@ljmu.ac.uk
* School of Engineering, Liverpool John Moores University, Byrom Street, Liverpool L3 3AF, UK

Abstract: Offshore floating wind turbines (FOWTs) operate under continuous platform motions that significantly influences rotor aerodynamics and wake development. In particular, surge motion alters the convection and spatial distribution of the helical vortex system, leading to complex wake interactions that are challenging to resolve using high-fidelity blade-resolved computational fluid dynamics (CFD) approaches. In the present study, a three-dimensional Actuator Line Model (ALM) is developed to investigate the unsteady wake dynamics of a FOWT undergoing prescribed harmonic surge motions. The rotor blades are represented by rotating actuator lines that introduce distributed body forces into the incompressible unsteady Reynolds-averaged Navier–Stokes (URANS) equations. Aerodynamic loading is computed for local relative flow velocities using tabulated airfoil polar data. A modified Prandtl tip-loss correction is incorporated to account for finite blade effects. The body force projection is regularised using a three-dimensional Gaussian kernel to ensure numerical stability and realistic force distribution. Prescribed surge motion is incorporated directly into the actuator line kinematics through user-defined functions (UDFs), enabling accurate implementation of platform induced rotor displacement. To efficiently resolve near wake vortex structures while maintaining a tractable computational cost, a locally refined overset mesh strategy is incorporated. The numerical framework is verified and validated against the NREL Phase VI experimental data. The results demonstrate that periodic surge motion alters convection characteristics of the helical vortex system, increasing mutual induction between adjacent vortex filaments, resulting in further wake deformation and meandering. The proposed ALM framework captures the dominant surge induced wake dynamics at a fraction of the computational cost of blade-resolved CFD, providing an efficient and robust tool for the analysis of floating wind turbine aerodynamics and wake behaviour.

Keywords: Floating Offshore Wind Turbines (FOWTs), Computational Fluid Dynamics, Vorticity, Actuator Line Model (ALM)

1. Introduction

Floating offshore wind turbines (FOWT) operate under platform motions induced by wind, waves, and coupled aero-hydro effects. In a wind turbine, the root vortex generates counter rotating motion in the wake, while tip vorticity shed from the blade boundary layer forms a coherent helical structure that propagates downstream [1]. Unlike fixed bottom turbines, floating rotors undergo platform motion relative to their wake, altering the stability and structure of the blade generated vortex system. Surge motion periodically displaces the rotor through its own wake, promoting vortex interaction, pairing, and breakdown, and thereby modifying turbulence characteristics in both the near and far wake. Instability becomes significant when adjacent helical vortex filaments interact strongly and undergo vortex pairing, preceding distortion and breakdown and enhancing turbulent mixing and kinetic energy transport across the shear layer [2]. The dynamics of vortex ring pairs are governed by collective convection and self-induced velocities arising from their circulation [3]. Contra rotating vortices induce separating velocities, while corotating circulations promotes paired motion. The balance between these mechanisms determines vortex stability until diffusion or instability disrupts the structure [3].

The vortex structure of a FOWT is a determinant of the power generation and structural integrity of wind farms [1, 2]. The near wake vortex structure refers to the structured helical tip vortices that shield the wake core from the surrounding wind [3], so that no kinetic energy from the ambient flow enters the wind speed deficit behind the rotor. As this flow transforms to the turbulent state, the downstream wake is triggered and produces circular features such as vortex pairing and leapfrogging, which are the driving mechanisms that create the breakdown of organised helical tip vortex structures [4]. Surge motion evidently has the highest impact on the real operational conditions of a FOWT [5]. As the motion occurs in the same direction as the incoming wind, it generates the most significant aerodynamic responses, such as periodic fluctuations that are produced in the relative velocity seen at the rotor [1, 6]. The investigation of the rotor and wake interactions is vital in the examination of FOWT as it can force the turbine into states such as vortex ring state (VSR) or propeller state, both of which are extreme states where the platform structure moves faster than the incoming wind [6].

Blade element momentum theory (BEM) has been adopted in the past for the assessment of wind turbines because of its simplicity and low computational cost [7, 8]. The technique allows for the calculation of power and the main loads that occur due to the rotating blades. The theory is based on integrating both lift and drag values on isolated blade sections to calculate the different rotor loads [9]. However, this model is unable to model complex wake and inflow critically for the analysis of vortex structure, as it cannot truly capture the complex 3D helical system [1]. Whereas high fidelity blade resolved CFD can capture these unsteady dynamics but becomes computationally prohibitive under six degrees of motion. The Actuator Line Model (ALM) provides an efficient alternative by representing blade forces as distributed momentum sources, capturing large scale wake structures and tip vortex evolution. Despite extensive numerical and theoretical studies, experimental investigations of helical vortex instability in floating wind turbine wakes remain limited [8]. Although the aerodynamic and hydrodynamic responses to platform motions have been studied, a clear gap remains in the detailed modelling and understanding of wake dynamics. Limited research has focused on the stability of the wake under platform movement, specifically under each DOF, and how vortical structures within the wake interact and potentially destabilise under this motion. Further research is needed to fully understand the aerodynamic response of the rotor under these conditions. In the case of FOWTs, the wake effects create more complex flows due to the movements of the turbines and the interaction between the rotor and wake flows, with the effects of wake creating the biggest challenges in large scale floating wind farms, resulting in power loss and increased fatigue loads [10].

Sorensen, J. & Shen, W.Z. [19] introduced the Actuator Line Method (ALM) and created a suitable way to capture the unsteady wake development without the incorporation of full turbine blade geometry, allowing the resolution of distinct tip vortices and verification of the basic assumptions on the BEM method. Since the creation of this model, other authors have produced various models. Melani et al. employed the ALM in ANSYS Fluent to investigate its ability to resolve blade tip vortices . They compared a standard ALM with a "frozen" ALM where the forces were extracted directly from a blade-resolved CFD simulation to isolate the effects of force projection and flow sampling. By assessing different Gaussian kernels and the Line Average sampling technique, they found that progressively reducing the sampling considerably improved the prediction of spanwise loads and concluded that ALM can capture 3D tip effects. Ivanell et al. investigated the spatial stability of helical tip vortices[17]. In their research they creatied a fundamental framework for understanding vortex behaviour under the axial disturbances shown in surge motion. Although the paper focuses on a fixed bottom case, the conclusions relating to vortex stability under the displacements give a base for the study of surge motion in floating turbines. The findings imply that axial perturbations like those experienced by a platform under surge motion can trigger instabilities at specific critical frequencies, ultimately dictating the stability of the near wake and its transition to chaotic turbulent state. Sarmast et al. produced a vital investigation on how wind turbine wakes break down by analysing the stability of tip vortices using Large Eddy Simulation (LES) and ALM [11]. Their finding concluded that mutual inductance instability is the main driver of wake disintegration and leads to local vortex pairing or leapfrogging. Building on these ideas, Wang et al. (2024) looked at the evolution of FOWTs' wake characteristics under surge motion by combining ALM with Unsteady Reynolds-Averaged Navier-Stokes (URANS). Both papers provide the theory between fundamental vortex stability theory and how this may be applied to offshore applications, necessary for modelling complex wake interaction [10, 11].

Arabgolarcheh et al. used the ALM method with the k-ε turbulence model to assess the effect that platform motion has on the energy harvesting potential in large scale farms [1]. The approach was accurate while being computationally affordable and was verified against turbines with vast available wind data. Arabgolarcheh et al. illustrated reliability and numerical independence in the work and prove that an ALM formulation remains robust against numerical errors, thus allowing for the high-fidelity capture of non-linear phenomena like vortex pairing and wake breakdown [1]. ALM can consider tip effects without any additional corrections if the correct angle of attack sampling and force projection strategies have been included [10]. This work looks to further examine the vortex structure of the wake shed by FOWT, as vortex interaction, such as leapfrogging, can result in highly unsteady fluid motion [12].

The main purpose of this work is to investigate the unsteady wake dynamics of a floating wind turbine undergoing prescribed surge motion using a three-dimensional Actuator Line Model (ALM) and an overset mesh. The actuator line model has been developed by implementing a source term in the momentum equations. Dedicated UDFs (User Defined Function) are developed that introduce the actuator line model for blade and rotor motions.

2. Numerical Method

All computations were conducted using ANSYS Fluent 2025 R2, which was extended through custom user-defined functions to implement the actuator line methodology and floating-platform surge motion [13]. The k-ε method was adapted for computational efficiency and agreement with the benchmark paper. Reynolds number model is applied as no real geometry is adopted in the ALM framework, no accurate simulation of the blade's boundary layer is required [1].

The flow is governed by the incompressible, unsteady Navier–Stokes equations with a body-force source terms representing the actuator lines:

$$\rho(\frac{\partial \bar{u}}{\partial t} + \bar{u} \cdot \nabla \bar{u}) = -\nabla \bar{p} + \mu_{eff} \nabla^2 \bar{u} + S_{ALM}, \tag{1}$$

$$\mu_{eff} = \mu + \mu_t. \tag{2}$$

Where $\bar{u}, \bar{P}\ and\ \bar{\rho}$ Present the mean values of velocity, pressure and density respectively. μ is the kinematic viscosity, and S_{ALM} is the actuator line source term in the form of body forces. A similar source is used for the turbulence kinetic energy and dissipation rate equations. Flow field simulations have been carried out using incompressible URANS pressure-based solutions. The finite volume method was used to solve the governing equations.

2.1. Actuator Line Model Formulation

The actuator line model (ALM) models the turbine blades as rotating lines of momentum source in place of each blade inside the flow domain considering a projection width. A schematic of the actuator line methodology is presented in Figure 1. The source term S_{ALM} on the right-hand side of Eq. (1) represents the body force that artificially represents the blade section in an actuator line model. The aerodynamic forces are calculated and distributed onto the computational mesh. The body forces are gathered from the local flow conditions and airfoil characteristics and are spatially smeared using a regularisation kernel.

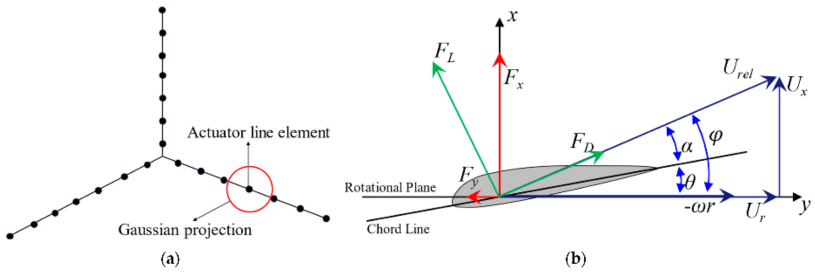

Figure 1- Diagram illustrating ALM method [13]

Although the blade geometry and boundary layers are not specifically resolved, the ALM allows for the generation of blade-induced vorticity as well as tip vortices, allowing the near and far wake structures of the turbine to be captured using reduced computational cost in comparison to blade resolved simulations[14]. In the ALM technique, each blade is represented by a rotating line discretised into spanwise segments. Each segment has a specific airfoil shape, twist, chord, and incoming wind kinematics. At each actuator point, the local relative velocity is computed as:

$$U_{rel} = U_{inflow} \times U_{rotational} - U_{platform.} \tag{3}$$

Where $U_{inflow}$is the incoming wind velocity, $U_{rotational}$ is the velocity induced on the rotor, and $U_{platform}$ the velocity due to platform translational surge motion. All these velocities are calculated locally for each blade element. The angle of attack α is obtained locally from the relative velocity and blade pitch, and sectional lift and drag forces are evaluated using tabulated airfoil polars. The sectional lift and drag forces are projected onto the Cartesian momentum equations and distributed to the surrounding flow field using a three-dimensional Gaussian kernel:

$$S_{ALM}(x) = \sum_{i=1}^{N} F_{tip} \mathrm{F}_N \, \eta \tag{4}$$

In the above equation, F_N represent the force at actuator element N calculated from lift and drag forces. These forces are calculated for tabulated airfoil data considering local angles and relative wind speeds.

The sectional lift and drag forces are computed as:

$$L = \frac{1}{2}\rho V_{rel}^2 c C_L \Delta r \tag{5}$$

$$D = \frac{1}{2}\rho V_{rel}^2 c C_D \Delta r \, , \tag{6}$$

where $V_{rel}$is the relative velocity magnitude, c is the local chord length, $C_L$and $C_D$are the lift and drag coefficients, and $\Delta r$is the blade element width.

The calculated aerodynamic forces are projected smoothly onto the flow field using the Gaussian function η as follows:

$$\eta = \frac{1}{\varepsilon^3 \pi^{3/2}} \exp(-\frac{|x - x_i|^2}{\varepsilon^2}). \tag{7}$$

The projection width of the Gaussian operation is determined by ε, chosen proportional to the local grid spacing to ensure numerical stability while preserving vortex coherence. In the current results, ε is set to 3 times the mesh spacing in the streamwise direction, i.e. $\varepsilon \cong 3\Delta x$. The Gaussian smearing prevents singular forcing and enables smooth coupling between the actuator lines and the resolved flow field. The airfoil polars are introduced in spanwise directions of the rotor, and the aerodynamic forces generated by the turbine are computed and distributed as body forces along the line elements that represent the blades. This technique allows implementation of the aerodynamic forces and corresponding changes without implementing a fully resolved geometry, resulting in a huge reduction in computational cost while still enabling the instantaneous vortical structures in the wake to be resolved and enabling detailed investigation of vortex interactions during surge motion of a floating wind turbine [15]. The implemented Prandtl tip-loss correction factor is shown in Eq. (8).

$$F = \frac{2}{\pi} cos^{-1} \left[\exp\left(-\frac{B}{2} \frac{R-r}{r \sin \emptyset} \right) \right]. \tag{8}$$

Where B is the number of blades, R is the rotor radius, r is the local radial position and ϕ is the inflow angle. In the absence of tip loss correction, the model will overpredict the thrust and wake deficit at the blade, as these value can be overestimated as they rely on 2D data and this model adjusts those numbers to match a 3D reality [16].

The selection of the time step size was governed by several physical and numerical considerations associated with the actuator line representation of the floating wind turbine and the transient wake dynamics during surge motion. In actuator line simulations, insufficient temporal refinement can lead to excessive smearing of the helical vortex structures generated by the blades [7]. Consequently, the temporal resolution is strongly coupled to the local grid spacing and rotor tip speed as well as platform motion frequencies. The time step size was selected to ensure adequate resolution of blade rotation, tip-vortex formation, and the resulting surge-induced evolution of the helical wake.

Two main criteria were used for time-step size selection in the fixed wind turbine simulation: the Courant–Friedrichs–Lewy (CFL) number and the blade azimuthal advancement per time step. The initial time-step size was selected to satisfy the CFL condition in the near wake region, which requires that the distance travelled by the flow during a single time step remain smaller than the characteristic cell size in the rotor region. In terms of blade azimuthal advancement, the time-step size was estimated using the criterion commonly adopted in actuator line methodologies, whereby the blade tip must not traverse more than one computational cell per time step [7]. Accordingly, the time step was set so that the actuator forcing distribution and the vortex shedding process are sufficiently resolved during each time step [1].

2.2. Computational Domain, Boundary Conditions and Meshing

The computational domain is shown in Figure *2* and includes dimensions of 10D, 3D and 4D in streamwise, spanwise and normal directions.

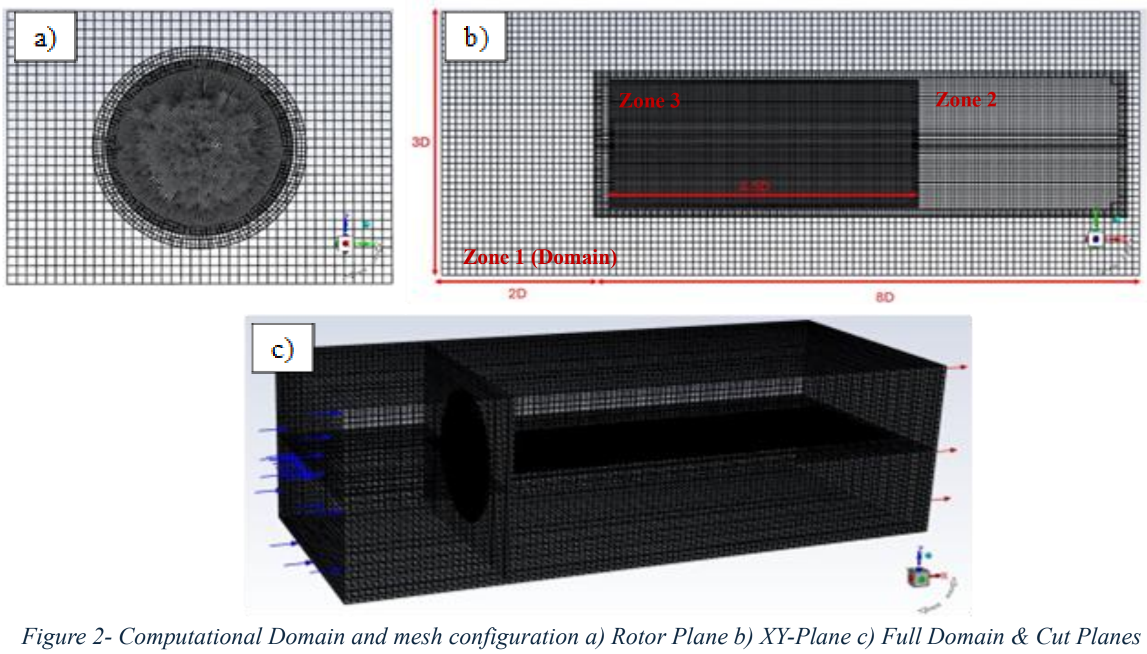

Figure 2- Computational Domain and mesh configuration a) Rotor Plane b) XY-Plane c) Full Domain & Cut Planes

The mesh has been concentrated around the actuator rotor projection area and wake area through the introduction of two cylinders around the plane of the disk, both refined respectively to ensure the capture of wake shed from the blades 'Zone 2' and 'Zone 3'. An overset mesh, i.e., Chimera method, was employed, using two cylindrical overset regions as shown in Figure *2,* where the ALM forces are projected. This approach was chosen over adaptive mesh refinement (AMR) because AMR can incur a run time penalty due to the computational effort of performing continuous refinements and maintaining processor load balancing [1]. The overset method allows for the implementation of submeshes that overlap and can move without the connectivity constraints or physical contact requirements seen in sliding mesh techniques [6]. As the ALM represents turbine blades as volumetric source terms projected onto the cells, it can be structured so that no physical mesh deformation is needed during the implementation of surge motion [17]. The interaction between each zone is managed through 'fringe cells' acting as a bridge between the overlapping areas, allowing for velocity and other flow properties to be accurately interpolated across the boundaries [6].

2.3. Platform motion

Platform surge motion is described as a harmonic displacement in the streamwise direction of the rotor:

$$x_s(t) = A_s si\,n(\omega_s t). \tag{9}$$

Where x_s is the surge motion rotor displacement, A_s and ω_s are the amplitude and frequency, respectively. The selected values for the surge case include a frequency of 0.59Hz and an amplitude of 0.63m. For this case, the NREL phase VI turbine was modelled in relation to the reference paper that adopts the NREL 5-MW turbine for the surge motion cases, both the frequency and amplitude have been adjusted in line with the turbine's properties. Within the reference literature, the amplitudes used in the case would create discrepancies within the work, as the parameters were chosen with exaggerated values to purposefully trigger various extreme cases, such as vortex ring state (VSR) [1]. By replicating a scaled amplitude of 0.63 m, the simulation keeps a reduced amplitude of 0.59, ensuring the turbine's travel remains proportional to its scale. When paired with a surge frequency of 0.597 Hz, which corresponds to a reduced frequency (relative to the 71.63 RPM rotor frequency), this setup ensures that one surge period equals exactly two rotor revolutions. The surge motion is incorporated directly into the actuator line kinematics by updating the rotor centre position and relative velocity at each time step. Similar temporal resolution requirements for floating offshore wind turbine wake simulations using actuator line models have also been reported in previous studies [18, 19].

3. Verification and Validation

The verification and validation are carried out for a stationary NREL Phase VI turbine. The parameters of this turbine and the operating conditions are shown in *Table 1*.

Parameter	Value
Blade Section Profile	S809
Angular velocity	7.501 rads/s
TSR	5.4
Tip pitch	3°
Rotor Radius	5.029m
U_∞	7m/s
No. of blades sections	40
Hub radius	0.508 m
Air density	1.23kg/m³

Table 1- NREL Phase VI Wind turbine Specifications and inputs used in the current study

The iterative convergence of each time step was attained with residuals reducing below 10^{-6}. During these simulations, the considered time steps are $\Delta t = \frac{1}{400\,\Omega}$, where Ω is the rotational speed of the rotor. Using this time step, the calculated CFL at the blade tip remains less than 0.5. The calculation terminated when the power coefficient remained unchanged, which is about 5 revolutions of the rotor.

A grid independence study has been conducted using power coefficient values of four different mesh sizes, as stated in *Table 2,* with cell sizes varying in systematic multiples of each case. The Gaussian smearing parameter used in Eq. (7) was set in line with the local rotor cell size as $\varepsilon = 3\Delta x$ for each case, ensuring that the cases keep a consistent force distribution across the refinement levels. The results of *Table 2* are plotted in Figure *3*. *Table 2* showcases the different cases adopted with Case A being chosen due to its accuracy and alignment with test data, with a total cell count of 1610453.

Case	**Zone 1 (m) (Domain)**	**Zone 2 (m)**	**Zone 3 (m) (rotor zone)**	C_p	**Total Cell Count**
A	2	0.5	0.25	0.33	1610453
B	2	0.75	0.2	0.34	2354496
C	2	0.75	0.25	0.29	1364392
D	2	0.75	0.5	0.20	402129

Table 2: Mesh independence study for mesh size [m] in each region, at each case.

As illustrated in Figure *3*, mesh independence is achieved for Case (A). Four meshes were generated by progressively refining the element size in the inner and rotor domain zones, providing total cell counts of approximately 0.4 million to 2.35 million. The C_p changed by 12.1% between Case C and Case A, but only 2.9% between Case A and Case B, despite B containing 46% more cells. Specifically, for ALM cases the grid must be fine enough (relative to the smoothing parameter, ϵ) to capture the force distributions and not too large so that tip vortices cannot be correctly captured.

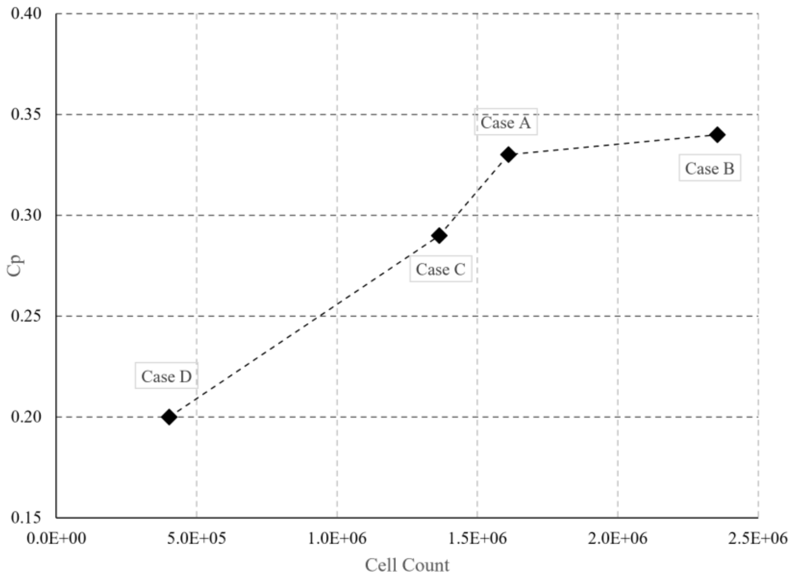

Figure 3- C_p independence study for total cell count

The results of fixed turbine are validated against NREL Phase VI turbine experimental data. This benchmark case is stall regulated and operates at a constant pitch and rotational speed, which allows researchers to focus on specific aerodynamic phenomena [20]. Ultimately, this validation gives the authors the confidence to extend work into complex environments where turbines will undergo platform motions.

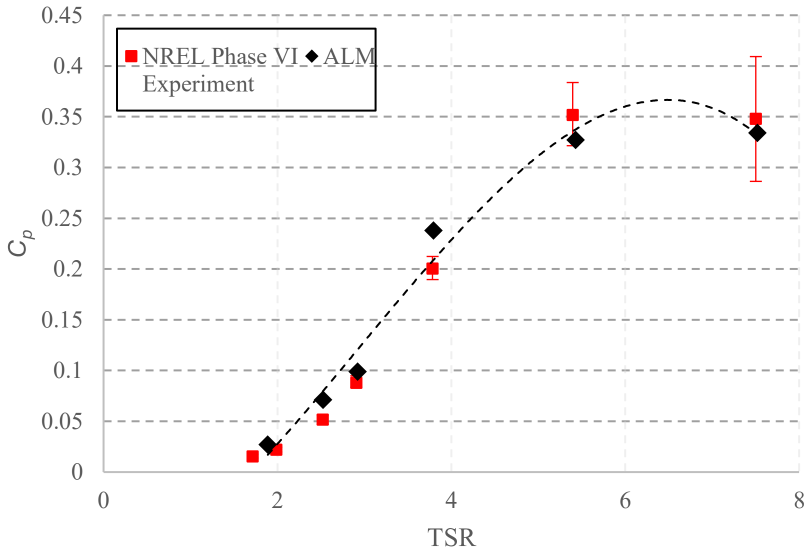

Figure 4- TSR against Cp for ALM code and NREL VI

The power coefficients are plotted in Figure 4 at a range of TSR for current simulation and experimental results. These results present a strong similarity between current results and experiments and provide sufficient evidence that this model can accurately predict the power coefficients for different TSRs.

4. Surge Motion Results

Harmonic platform surge motions presented in Eq. (9) are implemented to NERL Phase VI wind turbine at a tip speed ratio $\lambda = 7.501$ and a 3° pitch angle. The harmonic surge motion is considered at reduced frequency $F^* = 0.59$ and reduced amplitude $A^* = 0.63$. The reduced frequency and amplitude are normalised using the rotor frequency and diameter, respectively. A UDF is implemented for the calculation of three dimensional force sources on the actuator line. The lift and drag coefficients required for source term calculations were obtained from tabulated lift and drag coefficients corresponding to blade sections obtained from the experimental database [20]. Linear interpolation is employed between tabulated values within the ALM source term calculation at each time step.

In the absence of platform motion, the wake is characterised by a stable helical vortex system dominated by coherent tip vortices. When the same case is subjected to the surge motion, the relative displacement between the rotor and wake introduces a periodic modulation of vortex spacing and strength. As the rotor advances into regions of reduced axial velocity, adjacent helical filaments experience unsteadiness that accelerates vortex distortion and breakdown and promotes enhanced turbulent kinetic energy production, with the onset and intensity of the vortex interaction depending strongly on the surge amplitude and frequency. Overall, these results demonstrate that surge motion can fundamentally alter the vortex dynamics and stability of the wake; in the present case, the surge-induced unsteadiness accelerated the vortex breakdown.

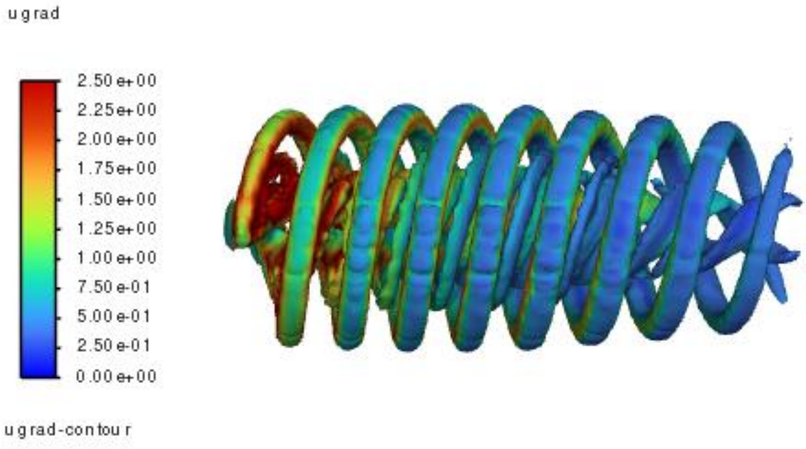

(a)

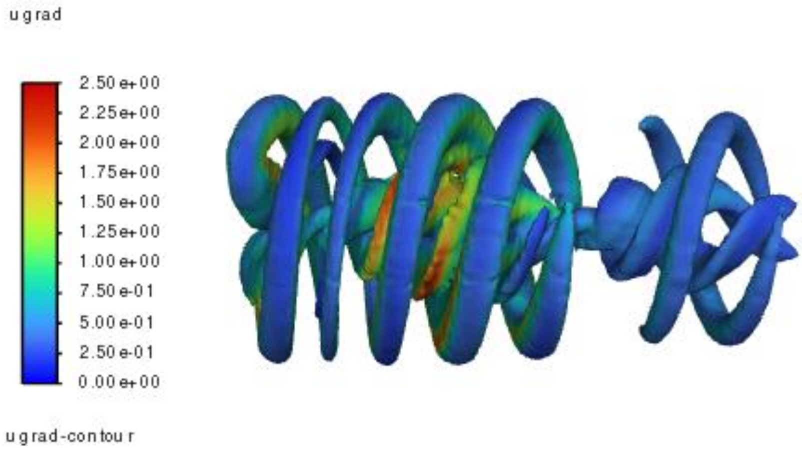

(b)

Figure 5- Iso-surface of Q=0.05 defined by Ugrad a) Fixed Case b) Surge Case F=0.59, A*=0.63*

5. Conclusions

In this paper, an actuator line model was developed for the simulation of the unsteady wake of floating offshore wind turbines during the surge motion. The simulation results of a fixed wind turbine were validated against the experimental measurements of the NREL Phase VI wind turbine. The platform motion results demonstrated that platform surge motion fundamentally perturbs the vortex dynamics and affects the stability of the wake structure. The periodic streamwise oscillation of the rotor introduced a cyclic variation in relative inflow velocity, which influenced the strength and formation of the tip vortices and promoted earlier vortex pairing compared to the fixed case, indicating that surge motion has an influence on downstream wake development and, therefore, on the performance of any turbines operating in the wake.

Future work will extend this study to surge motion across a range of amplitudes and frequencies, to characterise how these parameters govern the wake response. The findings will also be compared against further experimental datasets and alternative turbine configurations to establish how the results can be generalised beyond the NREL Phase VI case.

References

[1] A. Arabgolarcheh, S. Jannesarahmadi, and E. Benini, "Modeling of near wake characteristics in floating offshore wind turbines using an actuator line method," *Renewable Energy,* vol. 185, pp. 871–887, 2022, doi: 10.1016/j.renene.2021.12.099.

[2] H. C. Onel and I. H. Tuncer, "Investigation of wind turbine wakes and wake recovery in a tandem configuration using actuator line model with LES," *Computers & Fluids,* vol. 220, p. 104872, 2021, doi: 10.1016/j.compfluid.2021.104872.

[3] K. Brown, D. Houck, D. Maniaci, C. Westergaard, and C. Kelley, "Accelerated Wind-Turbine Wake Recovery Through Actuation of the Tip-Vortex Instability," *AIAA Journal,* vol. 60, no. 5, pp. 3298–3310, 2022, doi: 10.2514/1.J060772.

[4] L. Tophøj and H. Aref, "Instability of vortex pair leapfrogging," *Physics of Fluids,* vol. 25, no. 1, 2013.

[5] T. T. Tran and D.-H. Kim, "A CFD study into the influence of unsteady aerodynamic interference on wind turbine surge motion," *Renewable Energy,* vol. 90, pp. 204–228, 2016.

[6] R. Kyle, Y. C. Lee, and W.-G. Früh, "Propeller and vortex ring state for floating offshore wind turbines during surge," *Renewable Energy,* vol. 155, pp. 645–657, 2020, doi: 10.1016/j.renene.2020.03.105.

[7] J. N. r. Sørensen and W. Z. Shen, "Numerical Modeling of Wind Turbine Wakes," *Journal of Fluids Engineering,* vol. 124, no. 2, pp. 393–399, 2002, doi: 10.1115/1.1471361.

[8] X. Wang, C. Cai, S.-G. Cai, T. Wang, Z. Wang, J. Song, X. Rong, and Q. a. Li, "A review of aerodynamic and wake characteristics of floating offshore wind turbines," *Renewable and Sustainable Energy Reviews,* vol. 175, p. 113144, 2023, doi: 10.1016/j.rser.2022.113144.

[9] G. L. Ingram, "Wind Turbine Blade Analysis using the Blade Element Momentum Method. Version 1.1," 2011.

[10] T. Wang, C. Cai, J. Liu, C. Peng, Y. Wang, X. Sun, X. Zhong, J. Zhang, and Q. Li, "Wake characteristics and vortex structure evolution of floating offshore wind turbine under surge motion," *Energy,* vol. 302, p. 131788, 2024.

[11] S. Sarmast, R. Dadfar, R. F. Mikkelsen, P. Schlatter, S. Ivanell, Jens N. Sørensen, and Dan S. Henningson, "Mutual inductance instability of the tip vortices behind a wind turbine," *Journal of Fluid Mechanics,* vol. 755, pp. 705–731, 2014, doi: 10.1017/jfm.2014.326.

[12] P. Weidman and N. Riley, "Vortex ring pairs: numerical simulation and experiment," *Journal of Fluid Mechanics,* vol. 257, pp. 311–337, 1993.

[13] J. Xin, Y. Lai, Y. Yang, L. Tang, and S. Chen, "Actuator Line Wall-Modeled Immersed Boundary Method for Predicting the Aerodynamic Performance of Wind Turbines," *Sustainability,* vol. 17, no. 23, p. 10498, 2025, doi: 10.3390/su172310498.

[14] D. Zhao, N. Han, E. Goh, J. Cater, and A. Reinecke, *Wind turbines and aerodynamics energy harvesters*. Academic Press, 2019.

[15] T. Li, Y. Zhang, Q. Yang, X. Zhou, Z. Zhang, and T. Wang, "Unsteady aerodynamic characteristics of a floating offshore wind turbine in propeller state," *Renewable Energy,* vol. 246, p. 122861, 2025.

[16] W. Zhong, W. Z. Shen, T. Wang, and Y. Li, "A tip loss correction model for wind turbine aerodynamic performance prediction," *Renewable Energy,* vol. 147, no. P1, pp. 223–238, 2020, doi: 10.1016/j.renene.2019.08.125.

[17] S. Ivanell, R. Mikkelsen, J. N. Sørensen, and D. Henningson, "Stability analysis of the tip vortices of a wind turbine," *Wind Energy,* vol. 13, no. 8, pp. 705–715, 2010.

[18] A. Arab, S. Jannesarahamdi, and E. Benini, "Modeling of Near Wake Characteristics in Floating Offshore Wind Turbines Using an Actuator Line Method," *Renewable Energy,* vol. 179, pp. pp. 1407–1423, 2021.

[19] J. N. Sørensen and R. Mikkelsen, "Simulation of Wind Turbine Wakes Using the Actuator Line Technique," *Philosophical Transactions of the Royal Society A, 373, 20140071,* 2015.

[20] M. M. Hand, D. A. Simms, L. J. Fingersh, D. W. Jager, J. R. Cotrell, S. Schreck, and S. M. Larwood, *Unsteady Aerodynamics Experiment Phase VI: Wind Tunnel Test Configurations and Available Data Campaigns*. 2001.